26. J. Henrich, *J. Econ. Behav. Org.* **53**, 3 (2004).
27. Materials and methods are available as supporting material on *Science* Online.
28. U. Fischbacher, S. Gächter, E. Fehr, *Econ. Lett.* **71**, 397 (2001).
29. R. Kurzban, D. Houser, *Proc. Natl. Acad. Sci. U.S.A.* **102**, 1803 (2005).
30. Figure S1 displays the exact flow in both directions between institutions from one period to the next.
31. H. P. Young, *Individual Strategy and Social Structure: An Evolutionary Theory of Institutions* (Princeton Univ. Press, Princeton, NJ, 1998).
32. A logistic regression shows that the stay duration in SI in terms of the number of periods has a significantly negative influence on the likelihood of punishing others (table S1). Note, however, that individually exerted punishment may be lowered over time to effectively punish a free-rider because the number of potential punishers becomes larger. Indeed, average payoffs of free-riders decrease over periods, as can be seen from fig. S2.
33. In the last 10 periods, subjects who contribute highly and punish reach on average 98.7% of the payoff of subjects who contribute highly but do not punish.
34. C. Camerer, E. Fehr, *Science* **311**, 47 (2006).

35. We thank S. Bowles, E. Fehr, U. Fischbacher, S. Gächter, H. Gintis, G. Harrison, J. Henrich, M. Peacock, and R. Selten for helpful comments.

Supporting Online Material
www.sciencemag.org/cgi/content/full/312/5770/108/DC1
Materials and Methods
Figs. S1 and S2
Table S1
References

9 December 2005; accepted 14 February 2006
10.1126/science.1123633

Darwinian Evolution Can Follow Only Very Few Mutational Paths to Fitter Proteins

Daniel M. Weinreich,* Nigel F. Delaney,† Mark A. DePristo, Daniel L. Hartl

Five point mutations in a particular β-lactamase allele jointly increase bacterial resistance to a clinically important antibiotic by a factor of ~100,000. In principle, evolution to this high-resistance β-lactamase might follow any of the 120 mutational trajectories linking these alleles. However, we demonstrate that 102 trajectories are inaccessible to Darwinian selection and that many of the remaining trajectories have negligible probabilities of realization, because four of these five mutations fail to increase drug resistance in some combinations. Pervasive biophysical pleiotropy within the β-lactamase seems to be responsible, and because such pleiotropy appears to be a general property of missense mutations, we conclude that much protein evolution will be similarly constrained. This implies that the protein tape of life may be largely reproducible and even predictable.

Resistance to β-lactam antibiotics (e.g., penicillin) is commonly mediated by a bacterial β-lactamase, which hydrolytically inactivates these drugs (*1*). Bacterial resistance to novel β-lactams first arises by point mutations in the β-lactamase gene (*2*, *3*). Five point mutations in an allele of this gene that we designate TEM^{wt} (the reference sequence of the TEM family of β-lactamases) (*4*, *5*) jointly increase resistance by a factor of ~100,000 against cefotaxime (*6*, *7*), a third-generation cephalosporin β-lactam. These consist of four missense mutations [A42G, E104K, M182T, and G238S; numbering as in (*8*)] at clinically important residues (*3*, *9*) and one 5′ noncoding mutation [g4205a; numbering as in (*4*)], and we denote this high-resistance quintuple mutant *TEM**. Thus, five mutations must occur for *TEM** to evolve from TEM^{wt}, and because these can in principle occur in any order, there are 5! = 120 mutational trajectories linking these alleles. However, natural selection for heightened cefotaxime resistance may not regard all trajectories equivalently (*10*). Here, we determine the prevalence with which these mutations only conditionally increase drug resistance, a form of interaction previously designated sign epistasis (*10*). Sign epistasis is both necessary and sufficient for one or more trajectories to *TEM** to be selectively inaccessible (*10*).

To characterize the effect on drug resistance of each mutation on all allelic backgrounds, we first constructed the 32 combinations of these five mutations (*11*, *12*). We next determined their resistance to cefotaxime (*12*) in *Escherichia coli* strain DH5α (Table 1); because the sign of the mutational effect on drug resistance determines the selective accessibility of each trajectory (*10*), we also report the rank order of drug resistance values exhibited by all alleles. *TEM** exhibits the highest resistance and, because at least one mutation increases resistance in all other alleles, the fitness landscape is single-peaked (*13*). Thus, in the case of cefotaxime resistance evolution, populations cannot become trapped (*13*) at suboptimal alleles between TEM^{wt} and *TEM**, as was recently also shown for isopropylmalate dehydrogenase (IMDH) evolution from a nicotinamide adenine dinucleotide phosphate (NADP)–dependent form to a nicotinamide adenine dinucleotide (NAD)–dependent form (*14*).

To estimate the relative probabilities with which evolution by natural selection for heightened cefotaxime resistance will realize each of the 120 possible mutational trajectories from TEM^{wt} to *TEM**, we assumed that the time to fixation or loss of individual mutations is far less than the time between mutations [the "strong selection/weak mutation" model of (*15*)]. Thus, the relative probability of realizing any particular mutational trajectory is the product of the relative probabilities of its constituent mutations, because under our assumption the choice of each subsequent fixation is statistically independent of all previous fixations (*12*). Next, for each allele we partitioned all possible mutations into those that are beneficial, deleterious, or neutral with respect to cefotaxime resistance. The probability of

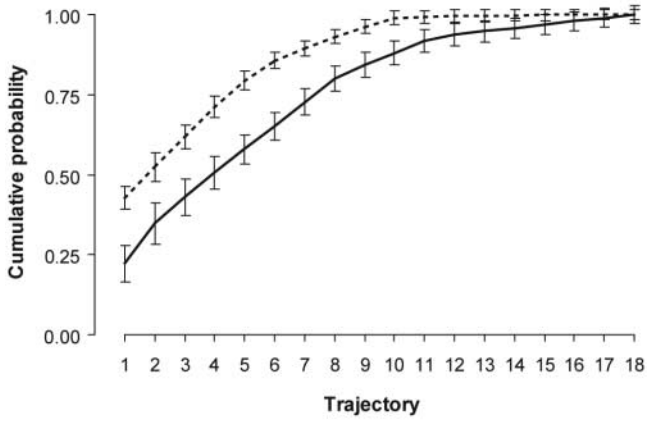

Fig. 1. Estimated cumulative probabilities for all 18 selectively accessible mutational trajectories from TEM^{wt} to *TEM**, under the correlated (broken line) and equal fixation probability (solid line) models, ± SEM. Trajectories are ordered in decreasing probability of realization.

Department of Organismic and Evolutionary Biology, Harvard University, 16 Divinity Avenue, Cambridge, MA 02138, USA.

*To whom correspondence should be addressed. E-mail: dmw@post.harvard.edu
†Present address: Integrative Oceanography Division, Scripps Institute of Oceanography, 9500 Gilman Drive, La Jolla, CA 92037, USA.

fixation for a beneficial mutation far exceeds that for deleterious or neutral mutations (*12*, *15*) and, because all alleles have one or more beneficial mutations (Table 1), we approximated the probability of fixation for all other mutations by zero.

Applying this population genetic reasoning (*12*) to the data in Table 1 reveals that 102 of the 120 mutational trajectories from TEM^{wt} to *TEM** are selectively inaccessible. Although these five mutations were chosen for their large joint phenotypic effect, this result is necessarily (*10*) a consequence of the fact that some of the mutations do not increase cefotaxime resistance on all allelic backgrounds. Rather, four mutations have negligible or even negative effects on drug resistance in some combinations. Under our model, the probability of fixation for such mutations on such backgrounds—and hence of those trajectories on which they occur—is zero. The number of alleles on which each mutation has a positive, negative, or negligible effect, together with the mean proportional increase in cefotaxime resistance of each, is reported in Table 2. This illustrates the incidence of sign epistasis in our data set: mutations that only conditionally increase phenotype [(*10*) and supporting online text].

The relative probabilities of realization among the 18 selectively accessible trajectories reflect the probabilities of fixation of their constituent (beneficial) mutations, which in turn depend on the ecological circumstances in which drug resistance evolves (*12*). The simplest model assumes that all available beneficial mutations fix with equal probability [see (*12*) for ecological interpretation]. A biologically more realistic picture assumes that the relative probability of fixation of beneficial mutations is positively correlated with magnitude of effect (*12*), and we employed extreme value theory (*12*, *15*, *16*) to provide intuition into the evolutionary consequences of such a correlation. Extreme value theory provides estimates of these relative probabilities largely independent of the underlying distribution of fitness effects (*16*).

The mean cumulative probabilities of the 18 selectively accessible trajectories under the equal and correlated fixation models are shown in Fig. 1; individual probabilities are presented in table S2. The sharp skew to the left indicates that only a few trajectories capture most of the probability density. For example, half of all evolutionary realizations will follow just four and two trajectories, respectively, under the equal and correlated fixation probability models. Because some correlation between a mutation's effect on resistance and its probability of fixation is likely (*17*), the biologically relevant number is probably closer to the lower value. Note that the results illustrated in Fig. 1 are largely robust to small, undetected differences in drug resistance (see supporting online text). Figure 2 illustrates the source of this bias at the level of the constituent beneficial mutations defining the 10 most probable trajectories, which represent, respectively, ~90% and ~99% of the probability density under the equal and correlated fixation probability models.

The skew in probabilities of realization among trajectories under the equal fixation probability model (Fig. 1) is by definition (*12*) entirely due to the structure of sign epistasis in Table 1. For example, mutations along the most likely trajectory under this model occur in the order G238S, E104K, A42G, M182T, g4205a. Reversing the order of the second and third mutations (G238S, A42G, E104K, M182T, g4205a) defines a second trajectory whose probability of realization under this model is reduced by a factor of three (table S2). This is because after the initial two fixations in the first trajectory, only one beneficial alternative exists, whereas three alternatives exist at that juncture in the second (Fig. 2), reducing the probability of each by one-third (eq. S5a). This effect differs from that due to unequal probabilities of fixation among alternative beneficial mutations (*18*), which gives rise to the modest difference between curves in Fig. 1.

Biochemical and biophysical considerations of β-lactamase offer some insight into the mechanistic origin of the sign epistasis underlying our results. For example, G238S on the TEM^{wt} background is known to enhance cefotaxime hydrolysis (*19*–*21*) but simultaneously to increase aggregation (*19*) and reduce thermodynamic stability of the enzyme (*20*, *22*). Conversely, M182T alone modestly reduces hydrolysis (*20*) while reducing aggregation (*19*) and increasing thermodynamic stability (*20*). Thus, intramolecular pleiotropy of M182T and G238S accounts for the fact that M182T exhibits sign epistasis: On TEM^{wt} it reduces (or at least has negligible effect on) cefotaxime resistance, but together with G238S it increases resistance (Table 1), because the double mutant enjoys increased hydrolysis (*20*) without loss of thermodynamic stability (*23*). The 5′ noncoding mutation g4205a also exhibits sign epistasis. Although it increases gene expression by a factor of ~2.5 (*6*, *7*), the mean effect on resistance of this mutation is much smaller, and it significantly increases resistance in at most 8 of 16 alleles (Table 2). The explanation may involve aggregation of β-lactamase (*23*, *24*): Because

Table 1. Cefotaxime resistance of TEM β-lactamase alleles. Assayed as minimum inhibitory concentration (MIC) (*12*); median value across three replicates shown in μg/ml.

Missense mutations					Without g4205a mutation		With g4205a mutation	
A42G	E104K	M182T	G238S	Clinical designation*	MIC	Rank	MIC	Rank
–	–	–	–	TEM-1	0.088†	13‡	0.088	13
–	–	–	+	TEM-19	1.4	9	1.4	9
–	–	+	–	TEM-135	0.063†§	14	0.088§	13
–	–	+	+	TEM-20	32	6	3.6×10^2	5
–	+	–	–	TEM-17	0.13‖	12	0.18	11
–	+	–	+	TEM-15	3.6×10^2	5	3.6×10^2	5
–	+	+	–	TEM-106	0.18‖	11	0.18	11
–	+	+	+	TEM-52	3.6×10^2	5	2.1×10^3	3
+	–	–	–	None	0.088	13	0.088	13
+	–	–	+	None	23	7	3.6×10^2	5
+	–	+	–	None	1.4	9	0.088	13
+	–	+	+	None	3.6×10^2	5	3.6×10^2	5
+	+	–	–	None	1.4	9	2.0	8
+	+	–	+	None	2.1×10^3¶	3	1.5×10^3¶	4
+	+	+	–	None	0.80	10	1.4	9
+	+	+	+	None	2.9×10^3	2	4.1×10^3	1#

*Of protein sequence; from (*3*). †These two values not significantly different after Bonferroni correction. ‡This allele here designated TEM^{wt}. §These two values not significantly different after Bonferroni correction. ‖These two values not significantly different after Bonferroni correction. ¶These two values not significantly different after Bonferroni correction. #This allele here designated *TEM**.

the fraction of molecules aggregated rises with protein concentration (*25*), missense mutations that reduce aggregation [e.g., (M182T)] (*19*) may be necessary to render g4205a beneficial. (Compare the effects of g4205a on A42G/E104K/G238S with that on A42G/E104K/M182T/G238S in Table 1.) Thus, here again, pleiotropy represents the mechanistic basis of sign epistasis.

Seen as an analysis of clinical cefotaxime resistance evolution, our treatment makes several simplifying assumptions about the mutational and selective processes. For example, we have disregarded horizontal gene transfer and have limited attention to only five mutations. Furthermore we have assumed that selection acts only to increase resistance to cefotaxime, whereas microbes are exposed to a spatial and temporal diversity of antibiotic compounds in nature as well as in clinical settings (*1*). The implications of relaxing these assumptions are explored in the supporting online text.

However, this work was intended to answer a more fundamental evolutionary question: Given a set of point mutations known jointly to increase organismal fitness, how does Darwinian selection regard the many mutational trajectories available? The foregoing limitations notwithstanding, the implications of our study for this broader question are clear: When selection acts on TEM^{wt} to increase cefotaxime resistance, only a very small fraction of trajectories to *TEM** are likely to be realized, owing to sign epistasis mediated by intramolecular pleiotropic effects. Moreover, inasmuch as intramolecular pleiotropy (*11*, *25*) and concomitant sign epistasis are characteristic of many missense mutations (*25*), constraints on the selective choice of trajectories like those seen here are likely to apply to the evolution of other proteins. For example, application of our population genetic model to the fitness landscape between an engineered NADP- and the wild-type NAD-dependent forms of IMDH (*12*, *14*, *26*) reveals that at most 29% of all mutational trajectories are selectively accessible (supporting online text). Our conclusion is also consistent with results from prospective experimental evolution studies, in which replicate evolutionary realizations have been observed to follow largely identical mutational trajectories (*27*). However, the retrospective, combinatorial strategy employed here (*11*) substantially enriches our understanding of the process of molecular evolution because it enables us to characterize all mutational trajectories, including those with a vanishingly small probability of realization [which is otherwise impractical (*27*)]. This is important because it draws attention to the mechanistic basis of selective inaccessibility. It now appears that intramolecular interactions render many mutational trajectories selectively inaccessible, which implies that replaying the protein tape of life (*28*) might be surprisingly repetitive. It remains to be seen whether intermolecular interactions similarly constrain Darwinian evolution at larger scales of biological organization.

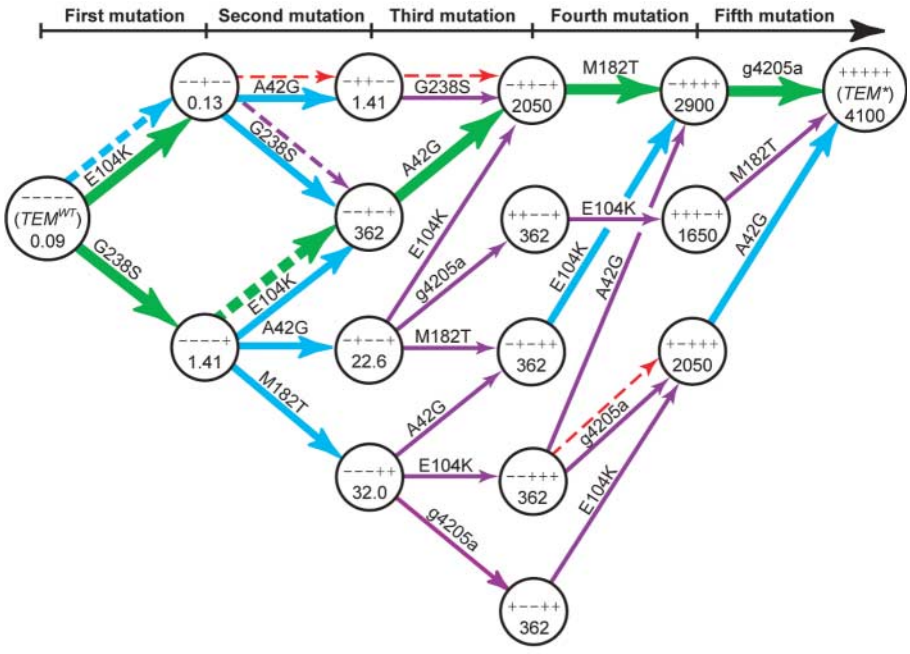

Fig. 2. Mutational composition of the 10 most probable trajectories from TEM^{wt} to *TEM**. Nodes represent alleles whose identities are given by a string of five + or – symbols corresponding (left to right) to the presence or absence of mutations g4205a, A42G, E104K, M182T, and G238S, respectively. Numbers indicate cefotaxime resistance (*12*) in μg/ml. Edges represent mutations, as labeled. The relative probability of each beneficial mutation is represented on a log scale by color and width of edges: green/wide, 0.316 to 1.0; purple/medium, 0.1 to 0.316; blue/narrow, 0.0316 to 0.1; and red/very narrow, less than 0.0316. Where two edges are shown between a pair of nodes, solid and broken edges correspond to probabilities under the equal and correlated fixation probability models, respectively. Elsewhere values differ between models by less than a factor of $\sqrt{10} = 0.316$.

Table 2. Summary of mutational effects on cefotaxime resistance.

Mutation	Number of TEM alleles on which mean mutational effect is			Mean† proportional increase
	Positive*	Negative*	Negligible	
g4205a	8‡	2‡	6	1.4
A42G	12	0	4	5.9
E104K	15	1	0	9.7
M182T	8‡	3‡	5	2.8
G238S	16	0	0	1.0×10^3

*Differences in mean MIC values are significant at $P < 0.05$. †Of MIC (*12*); geometric mean across all 16 alleles. ‡One of these comparisons loses significance after Bonferroni correction.

References and Notes

1. C. Walsh, *Antibiotics: Actions, Origins, Resistance* (American Society for Microbiology, Washington, DC, 2003).
2. A. A. Medeiros, *Clin. Infect. Dis.* **24**, S19 (1997).
3. G. A. Jacoby, K. Bush, *TEM Extended-Spectrum and Inhibitor Resistant* β-*Lactamases* (2005), www.lahey.org/Studies/temtable.asp.
4. N. Watson, *Genet. Anal. Tech. Appl.* **70**, 399 (1988).
5. B. G. Hall, M. Barlow, *Drug Resist. Updates* **7**, 111 (2004).
6. W. P. C. Stemmer, *Nature* **370**, 389 (1994).
7. B. G. Hall, *Antimicrob. Agents Chemother.* **46**, 3035 (2002).
8. R. P. Ambler *et al.*, *Biochem. J.* **276**, 269 (1991).
9. M. C. Orencia, J. S. Yoon, J. E. Ness, W. P. C. Stemmer, R. D. Stevens, *Nat. Struct. Biol.* **8**, 238 (2001).
10. D. M. Weinreich, R. A. Watson, L. Chao, *Evolution Int. J. Org. Evolution* **59**, 1165 (2005).
11. B. A. Malcolm, K. P. Wilson, B. W. Matthews, J. F. Kirsch, A. C. Wilson, *Nature* **345**, 86 (1990).
12. Materials and methods are available as supporting material on *Science* Online.
13. S. Wright, in *Proceedings of the Sixth International Congress of Genetics*, D. F. Jones, Ed. (Brooklyn Botanic Garden, Menasha, WI, 1932), pp. 356–366.
14. M. Lunzer, S. P. Miller, R. Felsheim, A. M. Dean, *Science* **310**, 499 (2005).
15. J. H. Gillespie, *Evolution Int. J. Org. Evolution* **38**, 1116 (1984).
16. H. A. Orr, *Evolution Int. J. Org. Evolution* **56**, 1317 (2002).
17. M. Barlow, B. G. Hall, *Genetics* **160**, 823 (2002).
18. H. A. Orr, *Evolution Int. J. Org. Evolution* **59**, 216 (2005).
19. V. Sideraki, W. Huang, T. Palzkill, H. F. Gilbert, *Proc. Natl. Acad. Sci. U.S.A.* **98**, 283 (2001).

20. X. Wang, G. Minasov, B. K. Shoichet, *J. Mol. Biol.* **320**, 85 (2002).
21. X. Raquet *et al.*, *J. Mol. Biol.* **244**, 625 (1994).
22. X. Raquet *et al.*, *Proteins* **23**, 63 (1995).
23. W. Huang, T. Palzkill, *Proc. Natl. Acad. Sci. U.S.A.* **94**, 8801 (1997).
24. G. Georgiou, P. Valax, M. Ostermeier, P. M. Horowitz, *Protein Sci.* **3**, 1953 (1994).
25. M. A. DePristo, D. M. Weinreich, D. L. Hartl, *Nat. Rev. Genet.* **6**, 678 (2005).
26. Data provided by A. M. Dean.
27. H. A. Orr, *Nat. Rev. Genet.* **6**, 119 (2005).
28. S. J. Gould, *Wonderful Life: The Burgess Shale and the Nature of History* (W. W. Norton and Company, New York, 1989).
29. M. Barlow and B. Hall introduced us to the TEM β-lactamase system and shared expertise and reagents with us. N. Shoresh suggested use of the likelihood framework and computed the critical values for the likelihood ratio test. D.M.W. and N.F.D. were supported by NSF under award DEB-0343598. M.A.D. is a Damon Runyon Fellow supported by the Damon Runyon Cancer Research Foundation (DRG-1861-05).

Supporting Online Material
www.sciencemag.org/cgi/content/full/312/5770/111/DC1
Materials and Methods
SOM Text
Fig. S1
Tables S1 and S2
References and Notes

7 December 2005; accepted 28 February 2006
10.1126/science.1123539

Naïve and Memory CD4+ T Cell Survival Controlled by Clonal Abundance

Jason Hataye,[1]* James J. Moon,[1] Alexander Khoruts,[2] Cavan Reilly,[3] Marc K. Jenkins[1]

Immunity to a plethora of microbes depends on a diverse repertoire of naïve lymphocytes and the production of long-lived memory cells. We present evidence here that low clonal abundance in a polyclonal repertoire favors the survival and activation of naïve CD4+ T cells as well as the survival of their memory cell progeny. The inverse relation between clonal frequency and survival suggests that intraclonal competition could help maintain an optimally diverse repertoire of T cells and an optimal environment for the generation of long-lived memory cells.

Protective immunity against infectious disease depends on antigen-specific memory T cells that survive for many years following initial exposure to antigen (*1*). One major paradigm, based largely on studies of CD8+ T cells, suggests that memory results from the conversion of naïve cells to long-lived memory cells that self-renew through the actions of the cytokine interleukin-15 (IL-15) (*1*). However, this mechanism may not apply to memory CD4+ T cells because they are less dependent on IL-15 and may be derived from naïve precursors that are themselves long-lived (*1*). Furthermore, polyclonal virus–specific memory CD4+ T cells have been seen to decline for almost a year after infection, indicating that not all memory CD4+ T cells are stably maintained (*2*). Such discrepancies prompted us to study the stability of naïve and memory CD4+ T cell populations.

To assess the in vivo survival of polyclonal naïve CD4+ T cells, CD44low CD4+ cells from mice positive for the CD90.1 marker were tracked using antibodies to CD90.1 after adoptive transfer into congenic CD90.2+ recipients (*3*). During the first 2 months, the transferred naïve CD4+ T cells declined in the secondary lymphoid organs or blood of recipient mice with an estimated 50-day half-life (Fig. 1) (*4*), as reported by others (*5*, *6*). However, a longer observation period revealed an overall half-life estimate of 124 days, with 10% of the cells still remaining 1 year after transfer.

The survival time of transferred polyclonal naïve CD4+ T cells was probably underestimated with this approach because of the loss of some CD44low cells as a result of participation in immune responses to unknown foreign antigens. It was therefore necessary to test the survival of monoclonal naïve CD4+ T cells that could not be unintentionally activated by foreign antigen. Monoclonal populations of CD4+ T cells from ovalbumin peptide-I-A^d–specific DO11.10 (*7*) or flagellin peptide-I-A^b–specific SM1 (*8*) T cell antigen receptor (TCR) transgenic mice were used for this purpose. One million naïve DO11.10 or 4 × 10^6 SM1 CD4+ T cells were transferred intravenously into histocompatible BALB/c or C57BL/6 mice, respectively, resulting in the seeding of about 10^5 cells in the spleen and lymph nodes (Fig. 2A and Fig. 3, A and B). The monoclonal cells then declined with half-lives of 12 and 7 days, respectively (Fig. 3A, triangles, and Fig. 3B, diamonds), revealing them to be short-lived as compared with their polyclonal counterparts. The poor survival of transferred naïve TCR transgenic cells was not related to rejection because potential sensitization of recipient mice by one injection of transgenic cells did not cause a second inoculum of transgenic cells to disappear more quickly (fig. S1).

The increased survival of polyclonal compared with monoclonal naïve CD4+ T cells could have been related to clone size. The polyclonal repertoire of naïve T cells in a normal adult mouse is composed of about 2 × 10^6 unique clones of 50 cells each (*9*, *10*). Thus, 10^5 transferred monoclonal cells represents a clone size of ~2000 times that of the typical naïve clonal population. However, the conventional approach of sampling a small fraction of secondary lymphoid tissue to enumerate adoptively transferred T cells was inadequate to detect the 100 cells seeded by a 1000-cell transfer (Fig. 2B) because the background was too high (Fig. 2C).

The conventional method was improved using a magnetic bead–based enrichment step that concentrated all of the transferred cells from the spleen and lymph nodes of individual mice (compare Fig. 2, A and D) into a small volume and reduced the number of contaminating recipient cells by a factor of several hundred. This enrichment method enabled detection of

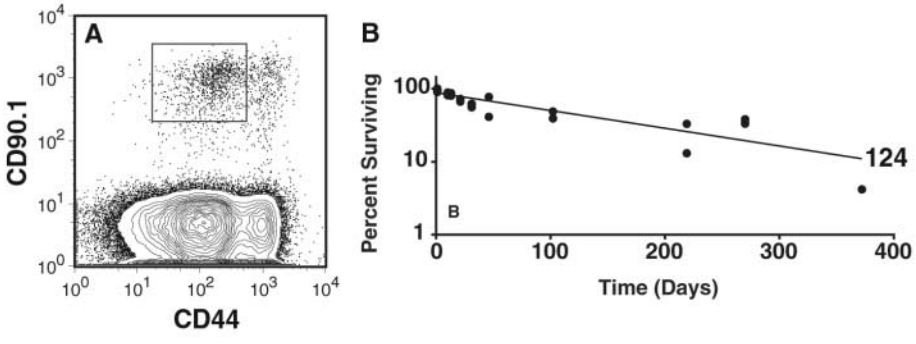

Fig. 1. Polyclonal naïve CD4+ T cells persist in normal recipients for more than 1 year. Two million polyclonal CD90.1+ CD4+ T cells were injected into CD90.2+ C57BL/6 mice. (**A**) The naïve transferred T cells were then identified as CD4+, B220− (not shown), CD90.1+, CD44low cells. (**B**) The percentage of these cells remaining in each recipient (pooled from two independent experiments) over time, fit to an exponential decay curve. The estimated half-life of the population (in days) is shown.

[1]Department of Microbiology, Center for Immunology, University of Minnesota Medical School, Minneapolis, MN 55455, USA. [2]Department of Medicine, Center for Immunology, University of Minnesota Medical School, Minneapolis, MN 55455, USA. [3]Division of Biostatistics, University of Minnesota School of Public Health, Minneapolis, MN 55455, USA.

*To whom correspondence should be addressed. E-mail: hata0006@umn.edu